Fault Classification and Voltage Sag Parameter Computation Using Voltage Ellipses

Juan Ramón Camarillo-Peñaranda and Gustavo Ramos

***Abstract*—Fault classification and voltage sag parameter computation using voltage ellipses in Clarke's domain are presented in this paper. The voltage sag parameters computed were the point-on-wave of initiation and recovery, residual voltage, and phase-angle jump. A change in the phase reference in Clarke's transformation was proposed to simplify the fault classification procedure. The point-on-wave of initiation and recovery were defined based on the reference circle in Clarke's domain, as described by the system during normal operation. The residual voltage and phase-angle jump were computed using the expressions of α and β components in Clarke's domain and trigonometric theorems. The proposed fault classification and voltage sag characteristics computation were applied to real data provided by the Department of Energy and the Electric Power Research Institute. From the results obtained, it is concluded that the zero-sequence component must be taken in consideration to compute the residual voltage and the phase-angle jump correctly, and to use these results to improve the accuracy of impedance-based fault location methods. The proposed fault classification algorithm is capable of classifying events and computing the residual voltage and phase-angle jump. Additionally, the voltage sag duration of short events and multistage events was successfully computed. This work is an incremental contribution within the field of voltage sag analysis in the time domain using Clarke's transformation.**

***Index Terms*—Fault detection, point-on-wave (POW), power quality (PQ) monitoring, unbalanced faults, voltage sags.**

I. Introduction

VOLTAGE sags are detrimental phenomena that affect sensitive industrial processes causing losses. A voltage sag study is important to predict the effect of the event on sensitive loads and industrial processes [1]. There is an interest in analyzing, classifying, and characterizing voltage sags because it is the most common power quality (PQ) disturbance. The most common approach to solve the voltage sag classification problem is the ABC classification proposed in [2]. This method is intuitive and easy to implement but ignore an important characteristic: the phase-angle jump. The work done by [3], [4] explains voltage sags and swells using a space vector approach, but the phase-angle jump and the point-on-wave (POW) characteristics were not addressed. For a complete voltage sag characterization, POW and phase-angle jump must be considered.

The work done by [5], [6] mainly focused on the effects of POW and phase-angle jump for sensitive equipment, including procedures for testing the tolerance of equipment to these voltage sag characteristics. The work done in [7], [8] was focused on computing POW and voltage sag characteristics from recorded data using the information of the three phases of the system. Neither of the mentioned authors considers the zero-sequence in their analysis. Not considering the zero-sequence in the analysis can lead to misinterpretations and loss of information, as it will be shown in the case study. This paper proposes Clarke's transformation-based method to classify and compute residual voltage, POW, and phase-angle jump from recorded data. The advantage to applying the proposed methodology was the reduction of the variables under consideration when computing the phase-angle jump and the voltage sag duration in the case of the POW of initiation and recovery. Additionally, by applying the proposed methodology, multistage events could be classified. This work shows the potential application of phase-angle jump in improving the accuracy of impedance-based fault location methods. The proposed voltage sag classification was suitable for an online application, and the result was obtained within one cycle.

II. Voltage Sag Classification

Clarke's transformation [9] was used to translate a three phase system, named V_{abc} into a system of two components: α and β, named $V_{\alpha\beta}$. This transformation was done by means of the $\mathbf{C}$ matrix shown in (1) [10]

$$[\mathbf{C}] = \sqrt{\frac{2}{3}}\begin{bmatrix} 1 & -\frac{1}{2} & -\frac{1}{2} \\ 0 & \frac{\sqrt{3}}{2} & -\frac{\sqrt{3}}{2} \end{bmatrix} \tag{1}$$

hence, the voltages in Clarke's domain are computed using

$$V_{\alpha\beta} = [\mathbf{C}]V_{abc} \tag{2}$$

In (2), $V_{\alpha\beta}$ and V_{abc} were column matrices that contain the α and β component and the three-phase voltages, respectively. As it was presented in [4], the shapes of the $\alpha\beta$ components plotted in a Cartesian system were ellipses in the case of unbalanced faults and circles in the case of normal operation and balanced faults. In [4, Table II], the following was observed.

1) The one phase to ground faults conserved the prefault amplitude in the β component.

Manuscript received January 27, 2018; revised July 7, 2018; accepted August 2, 2018. Date of publication August 6, 2018; date of current version December 12, 2018. Paper 2018-PSEC-0160.R1, presented at the 54th Industrial and Commercial Power Systems, Niagara Falls, ON Canada, May 7–10, and approved for publication in the IEEE Transactions on Industry Applications by the Power Systems Engineering Committee of the IEEE Industry Applications Society. This work was supported by COLCIENCIAS and Department of Cesar under the doctoral scholarship 014-681. *(Corresponding author: Juan Ramón Camarillo-Peñaranda.)*

The authors are with the Department of Electrical and Electronic Engineering, Universidad de los Andes, Bogotá 111711, Colombia (e-mail: jr.camarillo@uniandes.edu.co; gramos@uniandes.edu.co).

Digital Object Identifier 10.1109/TIA.2018.2864108

2) The two-phase faults conserved the prefault amplitude in the α component.
3) The two-phase to ground faults changed the value in both α and β components but were each different.
4) The balanced fault changed in both α and β components, equally.

Using the observations above, a simple fault classification algorithm can be implemented, but there is still an issue: the computation of the inclination angle of the ellipses. This issue was addressed in detail in [11], where a change in the reference of Clarke's transformation was presented. Given Clarke's transformation reference change, a fault classification algorithm could be accomplished. The fault classification algorithm was presented in [11]. The proposed algorithm can be implemented online, and the maximum time for a result is half a cycle.

III. POW and Voltage Sag Duration Computation

Two important characteristics of voltage sags are the POW of sag initiation and POW of sag recovery. These two voltage sag characteristics are important because each is useful in determining equipment sensitivity, and the exact voltage sag duration [5], [8]. The $\alpha\beta$ components also assist in computing the POW characteristics easily, but for the computation of these characteristics, only Clarke's transformation referenced in phase a (2) is used.

The POW of sag initiation can be defined as the angle at which the circle begins to deviate from its normal trajectory and turn into an ellipse. Similarly, the POW of sag recovery can be defined as the angle at which the fault ellipse begins to deviate from its trajectory and turn into a circle. Multistage and evolutionary voltage sags can also be described using the same reasoning. The voltage sag starts a new stage when the ellipse begins another change of shape, either into another ellipse or a circle. Implementing this approach allows for the classification of events with a duration of less than one cycle. In [11], several cases were shown to illustrate these observations.

IV. Phase Angle-Jump Computation Using Ellipses

Phase-angle jump is a phenomenon that affects the shape of ellipses in the $\alpha\beta$ framework, and therefore can be computed using ellipse parameters. In Figs. 1–3, three cases are shown, consisting of 50 (positive), zero, and -50 (negative) phase-angle jumps with different voltage sag depths. Values in the legend of Figs. 1–4 correspond to the sag depth. It can be concluded that positive phase-angle jump inclined ellipses to the right, negative phase-angle jump inclined the ellipses to the left, and zero phase-angle jump do not incline the ellipses. Moreover, for a fixed value of phase-angle jump, the intersection with the β axis was also fixed. Fig. 4 shows a zoomed-in version of the intersection of the ellipses with the positive β axis from Fig. 3. In fact, the value of the phase-angle jump can be computed from that zero intersection value, and in this case phase-angle jump $= \arccos(0.642482) = 50.0229$. The formal deduction of this method will be presented in the following paragraphs.

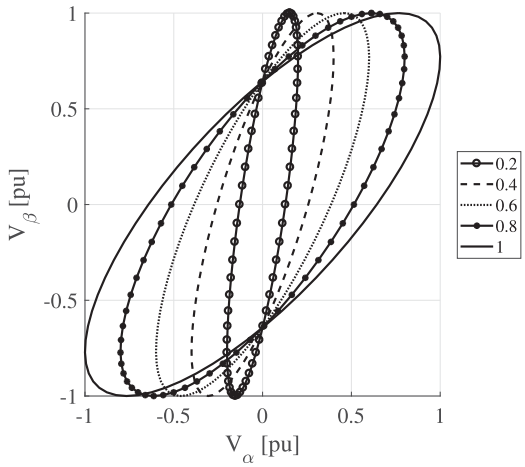

Fig. 1. Phase-angle jump = 50.

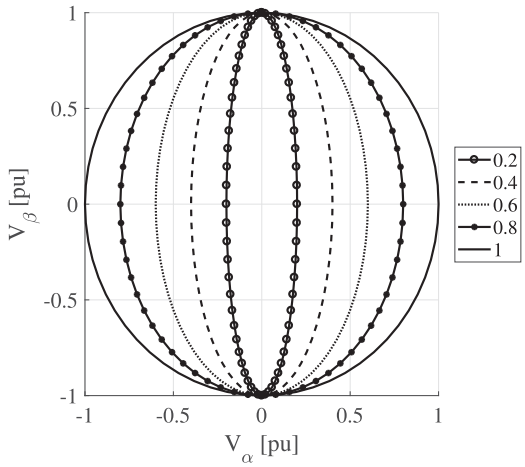

Fig. 2. Phase-angle jump = 0.

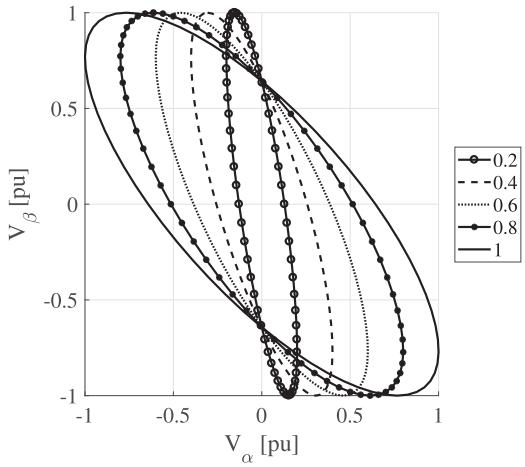

Fig. 3. Phase-angle jump = -50.

A. Symmetry in the β-axis

This case corresponds to a phase shift in the α component. The equations of the α and β components in this case are

$$V_\alpha(t) = A\cos(\omega t + \gamma)$$
$$V_\beta(t) = B\sin(\omega t) \tag{3}$$

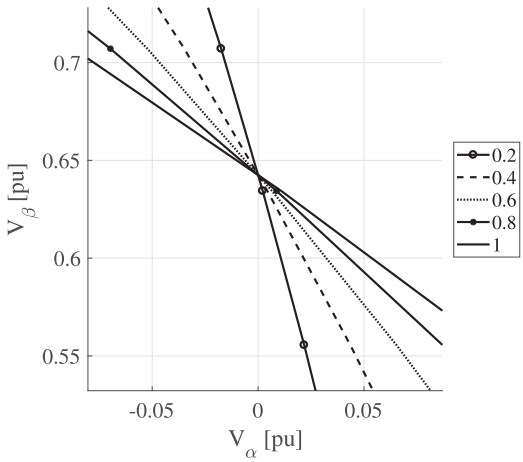

Fig. 4. Zoomed-in version of 3.

where γ is the phase-angle jump. The intersection with the β-axis occurs when the α component is equal to zero, i.e., $\omega t + \gamma = \frac{\pi}{2}$, or $\omega t = \frac{\pi}{2} - \gamma$. Replacing $\omega t = \frac{\pi}{2} - \gamma$ in the equation for the β component

$$V_\beta = B \sin\left(\frac{\pi}{2} - \gamma\right). \tag{4}$$

Applying the identity of the subtraction of angles results in

$$V_\beta = B\sin\left(\frac{\pi}{2}\right)\cos(\gamma) - B\sin(\gamma)\cos\left(\frac{\pi}{2}\right) \rightarrow V_\beta = B\cos(\gamma). \tag{5}$$

The phase-angle jump can be computed with

$$\gamma = \arccos\left(\frac{V_\beta}{B}\right). \tag{6}$$

In the case where $\omega t + \gamma = \frac{3\pi}{2}$, γ is computed as follows:

$$\gamma = \arccos\left(\frac{-V_\beta}{B}\right). \tag{7}$$

B. Symmetry in the α-Axis

This case corresponds to a phase shift in the β component. The equations of the α and β components are the following:

$$\begin{aligned} V_\alpha(t) &= A\cos(\omega t) \\ V_\beta(t) &= B\sin(\omega t + \gamma). \end{aligned} \tag{8}$$

The intersection with the α-axis occurs when the β component is equal to zero, i.e., $\omega t + \gamma = 0$, or $\omega t = -\gamma$. Replacing $\omega t = -\gamma$ in the equation of the α component

$$V_\alpha = A\cos(-\gamma). \tag{9}$$

Thus, the phase-angle jump can be computed with

$$\gamma = -\arccos\left(\frac{V_\alpha}{A}\right). \tag{10}$$

In the case where $\omega t = \pi - \gamma$, applying the identity of subtraction of angles results in

$$\begin{aligned} V_\alpha &= A\cos(\pi)\cos(-\gamma) + A\sin(\pi)\sin(-\gamma) \rightarrow V_\alpha \\ &= A\cos(-\gamma). \end{aligned} \tag{11}$$

The phase-angle jump can be computed with

$$\gamma = \arccos\left(\frac{V_\alpha}{A}\right). \tag{12}$$

Considerations: Since the cosine is an even function, the sign of the computed phase-angle jump cannot be determined by only using the result of (6), (7), (10), and (12). Thus, the following items must be taken into consideration to determine the sign of the phase-angle jump using the aforementioned deductions:

i) In the case of ellipses symmetric to the β-axis, if the value of the β component continues increasing (in absolute value) after crossing the β-axis, it can be concluded that the sign of the phase-angle jump is negative. In the converse scenario, it can be concluded that the sign of the phase-angle jump is positive.
ii) In the case of ellipses symmetric to the α-axis, if the value of the α component continues increasing (in absolute value) after crossing the α-axis, it can be concluded that the sign of the phase-angle jump is positive. In the converse scenario, it can be concluded that the sign of the phase-angle jump is negative.
iii) The absolute value of the phase-angle jump symmetric to β- and α-axes must be computed using (6) and (12), respectively, and the sign must be determined using the reasoning above.

Other considerations include the following.

i) The fault must be classified before the phase-angle jump is computed.
ii) The fault classification, phase-angle jump, and sag depth can be computed within half a cycle after the fault occurrence.

C. Balanced Fault

Assuming that the prefault system is balanced, the equations for the phase voltages are the following:

$$V_a(t) = AB\sqrt{2}\cos(\omega t + \phi) \tag{13}$$

$$V_b(t) = AB\sqrt{2}\cos\left(\omega t - \frac{2\pi}{3} + \phi\right) \tag{14}$$

$$V_c(t) = AB\sqrt{2}\cos\left(\omega t + \frac{2\pi}{3} + \phi\right) \tag{15}$$

where A is the RMS value of the phase voltage, B is the residual voltage, and ϕ is the phase-angle jump. Using these expressions, which are computed using (2), V_α and V_β are

$$\begin{aligned} V_\alpha(t) &= AB\sqrt{3}\cos(\omega t + \phi) \\ V_\beta(t) &= AB\sqrt{3}\sin(\omega t + \phi). \end{aligned} \tag{16}$$

From (16), it can be seen that both α and β components carry both the residual voltage and phase-angle jump. So, to compute the residual voltage, it is sufficient to use the maximum absolute value of either the α or β component. To compute the phase-angle jump, either the maximum value, the minimum value, or the axis intersection after the fault must be compared with the respective prefault value. If the time that the signal takes to reach a maximum/minimum/intersection during the fault is less

than one cycle, there is a positive phase-angle jump. For the converse, there is a negative phase-angle jump. Additionally, a frequency correction must be made, as in [7], to take into consideration the frequency variations during the operation of the system.

D. One Phase to Ground Faults

The equations for phase voltages in this fault are (in the case of a fault in phase a and a solidly grounded equivalent source)

$$V_a(t) = AB\sqrt{2}\cos(\omega t + \phi) \tag{17}$$

$$V_b(t) = A\sqrt{2}\cos\left(\omega t - \frac{2\pi}{3}\right) \tag{18}$$

$$V_c(t) = A\sqrt{2}\cos\left(\omega t + \frac{2\pi}{3}\right). \tag{19}$$

With these expressions, which are computed using (2), V_α and V_β are the following:

$$V_\alpha(t) = AB\frac{2\sqrt{3}}{3}\cos(\omega t + \phi) + A\frac{\sqrt{3}}{3}\cos(\omega t)$$
$$V_\beta(t) = A\sqrt{3}\sin(\omega t). \tag{20}$$

From (20), it can be seen that the resultant ellipses are symmetrical to the β axis; thus, the phase-angle jump can be computed using the methodology proposed in Section IV. However, in this case, the residual voltage and phase-angle jump cannot be computed directly by seeing the α component, because it is a summation of two sinusoids. The measurement equipment is the sum of the two sinusoids shown in (20), so to compute the residual voltage and the phase-angle jump, sine and cosine theorems must be applied. Let $M\cos\omega t + \theta$ be the sum of the two sinusoids in (20). Because of the factor $\sqrt{\frac{2}{3}}$ in Clarke's transformation matrix (1), a $\sqrt{3}$ factor must be applied. Using the cosine theorem and taking into consideration the $\sqrt{3}$ correction factor, the value of the residual voltage is computed as follows [11]:

$$\frac{4}{3}B^2 = \frac{1}{3} + (\sqrt{3}M)^2 - \frac{2\sqrt{3}}{3}\sqrt{3}M\cos(\theta) \tag{21}$$

$$4B^2 = 1 + 9M^2 - 6M\cos(\theta) \tag{22}$$

$$B^2 = \frac{1}{4} + \frac{9}{4}M^2 - \frac{3}{2}M\cos(\theta) \tag{23}$$

$$B = \sqrt{\frac{1}{4} + \frac{9}{4}M^2 - \frac{3}{2}M\cos(\theta)} \tag{24}$$

where M is the resisual voltage of the α component and θ is the phase-angle jump of the α component computed applying the methodology proposed in Section IV. Thus, to compute the residual voltage, (24) must be used. The sine theorem must be applied to compute the phase-angle jump as follows:

$$\frac{\frac{2\sqrt{3}}{3}B}{\sin(\theta)} = \frac{\frac{\sqrt{3}}{3}}{\sin(\phi - \theta)} \rightarrow \frac{2B}{\sin(\theta)} = \frac{1}{\sin(\phi - \theta)} \tag{25}$$

TABLE I
FAULT CLASSIFICATION FOR REAL DATA RECORDED BY DOE/EPRI

Signal	$V_{\alpha a}$	$V_{\beta a}$	$V_{\alpha b}$	$V_{\beta b}$	$V_{\alpha c}$	$V_{\beta c}$	Classification
2760	0.91	0.92	0.78	0.88	0.82	**1.00**	C2G
2797	0.85	0.90	0.92	**1.00**	0.88	0.86	A2G
2911	0.94	0.79	0.92	0.84	**1.00**	0.88	B2G
2912	0.94	0.79	0.92	0.84	**1.00**	0.87	B2G
2948	0.80	0.88	0.94	**1.00**	0.88	0.83	A2G
3235	**0.84**	**0.83**	**0.86**	**0.88**	**0.85**	**0.83**	ABC2G
3425	0.97	0.96	0.88	0.89	0.88	**1.00**	C2G
3552	0.95	0.84	0.94	0.83	**1.00**	0.87	B2G
3555	**1.00**	0.61	0.54	**0.31**	0.88	1.89	BC

The bold face indicate the values that lead to the classification shown in "Classification" column.

$$\sin(\phi - \theta) = \frac{\sin(\theta)}{2B} \tag{26}$$

$$\phi = \arcsin\frac{\sin(\theta)}{2B} + \theta. \tag{27}$$

Hence, to compute the phase-angle jump, (27) must be applied.

Considerations: The equations deduced above are valid only when the positive- and zero-sequence of the equivalent source are equal. In cases where this assumption does not hold, the zero-sequence component of Clarke transformation must be taken into consideration to compute the phase-angle jump and residual voltage, as it will be shown in the case study.

E. Two Phases to Ground Faults

The equations for phase voltages in this fault are

$$V_a(t) = A\sqrt{2}\cos(\omega t) \tag{28}$$

$$V_b(t) = AB\sqrt{2}\cos\left(\omega t - \frac{2\pi}{3} + \phi\right) \tag{29}$$

$$V_c(t) = AB\sqrt{2}\cos\left(\omega t + \frac{2\pi}{3} + \phi\right). \tag{30}$$

With this expressions, V_α and V_β are the following:

$$V_\alpha(t) = AB\frac{\sqrt{3}}{3}\cos(\omega t + \phi) + A\frac{2\sqrt{3}}{3}\cos(\omega t)$$
$$V_\beta(t) = AB\sqrt{3}\sin(\omega t + \phi). \tag{31}$$

From (31), it can be seen that the β component carries both the residual voltage and phase-angle jump. So, to compute the residual voltage, it is sufficient to use the maximum absolute value of the β component. For computing the phase-angle jump, the maximum value, the minimum value, or the intersection value after the fault must be compared with the respective prefault value. Then, a frequency correction must be applied to finally determine if there is a phase-angle jump during the fault.

F. Two Phase Fault

From [4], it can be observed that the α component in this fault does not change its value. Furthermore, from Table II, $B = M - N$ and the phase-angle jump can be included in the

TABLE II
POW AND VOLTAGE SAG DURATION FOR REAL DATA PROVIDED BY DOE/EPRI

Signal	POW initiation	POW recovery	Duration (cycles)
2760	44.19°	209.78°	1.46
2797	148.64°	???	???
2911	141.74°	284.21°	4.40
2912	251.03°	74.67°	5.51
2948	−5.87°	161.24°	4.54
3235	94.37°	28.16°	1.82
3425	39.74°	???	???
3552	112.00°	???	???
3555	70.43°	297.70°	2.63

??? means that the value cannot be computed. This happen because the signal has no point of recovery, and consequently, the duration cannot be computed.

equation as in the precedent cases. The α and β components in this fault are the following:

$$V_\alpha(t) = A\sqrt{3}\cos(\omega t)$$
$$V_\beta(t) = AB\sqrt{3}\sin(\omega t + \phi). \quad (32)$$

From (32), the resultant ellipses were symmetrical to the α axis; thus, the phase-angle jump can be computed using the methodology proposed in Section IV. The residual voltage is the same as during the event in the β component.

Considerations: The angle computed using the proposed approach is the difference between the phase-angle jump in the faulted phases. In other words, the $M - N$ difference is nonzero, which takes into consideration the difference between the X/R ratio of the line impedance and the equivalent source impedance. This fact allowed for the use of this result as an input to a fault location algorithm.

V. CASE STUDY

Real data provided by the Department of Energy (DOE) and the Electric Power Research Institute (EPRI) [12] were used to validate the proposed approach. The fundamental frequency of the recorded signals was 60 Hz.

A. Fault Classification

In Table I, the α and β components calculated for all phase references and respective fault classifications using the algorithm proposed in Section II are shown. The data used here were obtained from a DOE web page [12]. The results of Table I are consistent with previously published results [4], except for signal 3555. The corrected signal classification is the presented in Table I. The zero-sequence value during the fault was due to an unbalanced present before the fault inception.

B. POW and Voltage Sag Duration Computation

The proposed algorithm was also applied to DOE/EPRI signals, obtaining the results presented in Table II. The graphical representation for signals 2760 and 3555 is presented in Figs. 5 and 6.

In Figs. 5 and 6, the arrows pointing inside the figure indicate the POW of initiation, and the arrows pointing outside the figure indicate the POW of recovery. The signals are shown with no previous processing. The points of initiation and recovery and the event duration are quite evident from Figs. 5 and 6. These two signals have a relatively short duration; however, it was possible to compute the duration of the events. It is worth noting that the proposed methodology allows for the computation of the voltage sag duration of very short events, which is not possible or it is possible for a large error for some algorithms [13].

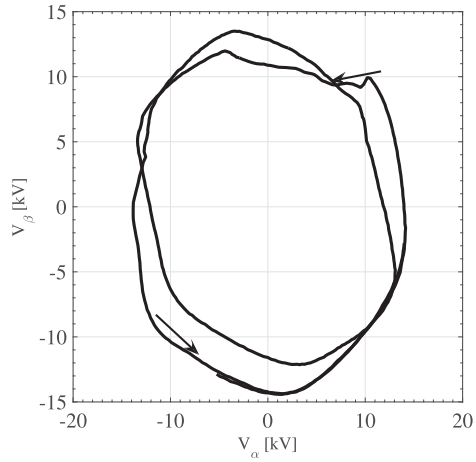

Fig. 5. POW and voltage sag duration for signal 2760.

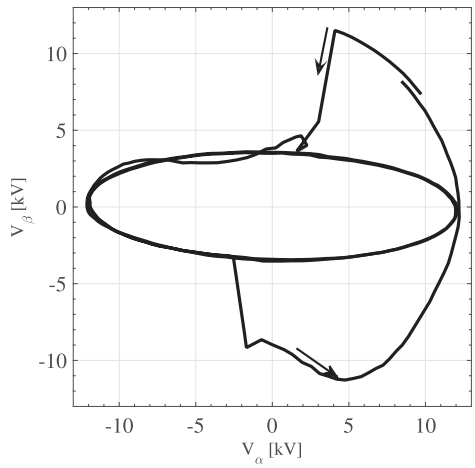

Fig. 6. POW and voltage sag duration for signal 3555.

C. Residual Voltage and Phase-Angle Jump Computation

It is possible to compute the residual voltage and phase-angle jump with the procedure presented in Section IV having completed the fault classification. These voltage sag parameters will be computed for the signals provided by DOE/EPRI.

The phase-angle jump and the residual voltage computed using the proposed methodology are shown in Table III. The graphical representation for signals 2911 and 2948 are shown in Figs. 7 and 8. In these figures, it can be observed that the 2911 and 2948 signals were referenced according to the fault classification of Table I. Table III presents the residual voltage and phase-angle jump computed directly from the signals and the proposed approach. From Table III, it can be observed that the residual voltage is computed with an acceptable error in all cases. For the computed phase-angle jump, the proposed

TABLE III
RESIDUAL VOLTAGE AND PHASE-ANGLE JUMP FOR REAL DATA RECORDED BY DOE/EPRI

Signal	Residual voltage	Phase-angle jump	β-cross	Computed residual voltage	Computed phase-angle jump
2760	0.78	14.06°	0.9986	0.74	−3.03°
2797	0.84	8.44°	0.9967	0.89	−4.66°
2911	0.79	28.13°	0.9838	0.71	−10.33°
2912	0.79	28.13°	0.9935	0.71	−6.54°
2948	0.80	33.75°	0.9819	0.70	10.92°
3235	0.85	0°	1.0000	0.88	0°
3425	0.85	15.63°	0.9964	0.90	−4.86°
3552	0.84	11.25°	0.9903	0.90	8.00°
3555	0.52	−5.63°	0.9915	0.47	−7.48°

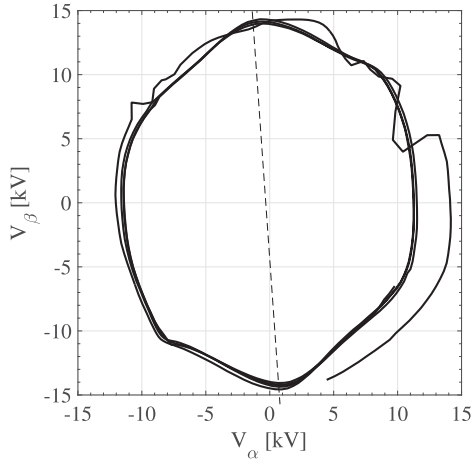

Fig. 7. During-fault ellipse for 2911 signal.

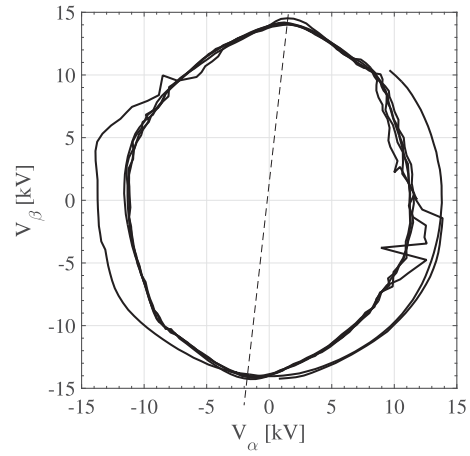

Fig. 8. During-fault ellipse for 2948 signal.

approach is quite good for the two phase fault (signal 3555). For the one-phase to ground faults, there is a systematic error in the computed value of the phase-angle jump. As it was mentioned in [4], these signals increase the value of the nonfaulted phases during the fault, likely due to a zero-sequence component in the model of the equivalent source. This zero-sequence component was not taken into consideration in the deductions of (24) and (27). Thus, to correct this issue, the zero-sequence component of Clarke's transformation must be taken into consideration. The zero-sequence component will be considered in fault location computations in the future.

VI. CONCLUSION AND FUTURE WORK

A fault classification and voltage sag parameters computation using voltage ellipses in Clarke's domain were presented in this paper. Procedures for computing the POW initiation and recovery, residual voltage, and phase-angle jump were shown. The proposed methodology was applied to real signals provided by DOE/EPRI. It was possible to classify the signals, precisely compute the voltage sag duration, and compute with some error the phase-angle jump and residual voltage. From the obtained results, it was shown the necessity of including the zero-sequence component in the phase-angle jump analysis. The zero-sequence component will help to compute the phase-angle jump correctly, and to improve the accuracy of impedance-based fault location methods potentially. Thus, ellipses formed with α and zero components and β and zero components will be considered in the future to complement the calculations shown in this paper.

In future work, the influence of transformers on the voltage sag classification will be analyzed. Additionally, the influence of imbalance and harmonics in the computation of the voltage sag parameters will be considered. The use of the presented voltage sag parameter computation in combination with some ellipse properties will be used for the computation of fault impedance and the location.

REFERENCES

[1] M. McGranaghan, D. Mueller, and M. Samotyj, "Voltage sags in industrial systems," in *Proc. Conf. Rec. Commercial Power Syst. Tech. Conf.*, May 1991, pp. 18–24.
[2] M. H. Bollen, "Voltage sags characterization," in *Understanding Power Quality Problems: Voltage Sags and Interruptions*. Hoboken, NJ, USA: Wiley, 2000, pp. 139–251.
[3] M. R. Alam, K. M. Muttaqi, and A. Bouzerdoum, "Characterizing voltage sags and swells using three-phase voltage ellipse parameters," *IEEE Trans. Ind. Appl.*, vol. 51, no. 4, pp. 2780–2790, Jul. 2015.
[4] J. R. Camarillo-Pearanda and G. Ramos, "Characterization of voltage sags due to faults in radial systems using three-phase voltage ellipse parameters," *IEEE Trans. Ind. Appl.*, vol. 54, no. 3, pp. 2032–2040, May 2018.
[5] S. Z. Djokic, J. V. Milanovi!c, and S. M. Rowland, "Advanced voltage sag characterisation ii: point on wave," *Transmiss. Distrib. IET Gener.*, vol. 1, no. 1, pp. 146–154, Jan. 2007.
[6] S. Z. Djokic and J. V. Milanovic, "Advanced voltage sag characterisation. Part I: Phase shift," *Transmiss. Distrib. IEE Proc. - Gener.*, vol. 153, no. 4, pp. 423–430, Jul. 2006.
[7] Y. Wang, M. H. J. Bollen, and X. Y. Xiao, "Calculation of the phase-angle-jump for voltage dips in three-phase systems," *IEEE Trans. Power Del.*, vol. 30, no. 1, pp. 480–487, Feb. 2015.
[8] Y. Wang, X.-Y. Xiao, and M. H. J. Bollen, "Challenges in the calculation methods of point-on-wave characteristics for voltage dips," in *Proc. 17th Int. Conf. Harmonics Quality Power*, Oct. 2016, pp. 513–517.
[9] E. Clarke, *Circuit Analysis of A-C Power Systems*. Hoboken, NJ, USA: Wiley, 1943.
[10] H. Akagi, E. H. Watanabe, and M. Aredes, "The instantaneous power theory," in *Instantaneous Power Theory and Applications to Power Conditioning*. Hoboken, NY, USA: Wiley, 2007, ch. 3, pp. 41–107, doi: 10.1002/9780470118931.
[11] J. R. Camarillo-Pearanda and G. Ramos, "Fault classification and voltage sag parameters computation using voltage ellipses," in *Proc. IEEE/IAS 54th Ind. Commercial Power Syst. Tech. Conf.*, May 2018, pp. 1–6.
[12] US Department of Energy and Electric Power Research Institute, "DOE disturbance library." Nov 2017. [Online]. Available: http://pqmon.epri.com/disturbance_librarysee_all.asp
[13] D. Gallo, C. Landi, and M. Luiso, "Accuracy analysis of algorithms adopted in voltage dip measurements," *IEEE Trans. Instrum. Meas.*, vol. 59, no. 10, pp. 2652–2659, Oct. 2010.

Authors' photographs and biographies not available at the time of publication.